JOURNAL OF APPLIED ELECTROCHEMISTRY 13 (1983) 377–382

*Polycrystalline In_2O_3 and In_2O_3/Y_2O_3 photoanodes**

F.-T. LIOU, C. Y. YANG, K. HAKIM

Department of Energy and Environment, Brookhaven National Laboratory, Upton, New York 11973, USA

S. N. LEVINE†

Department of Materials Science and Engineering, State University of New York at Stony Brook, New York 11790, USA

Received 28 July 1982

Single crystal In_2O_3 shows promise as a photoanode for the decomposition of water. Because of various difficulties in the preparation of the single crystal material, two simple techniques were developed for the preparation of polycrystalline In_2O_3 anodes. One method involves the thermal decomposition of the nitrate while the other utilizes the chemical vapour deposition technique. Voltammograms and photoresponse spectra of these anodes are compared to the single crystal material. Among other observations, it is noted that the quantum efficiencies of the thermally decomposed films are comparable to the single crystal material. It is also shown that the on-set potential can be shifted to more negative values by forming the mixed oxide In_2O_3/Y_2O_3.

1. Introduction

Recently McCann and Brockris [1] reported that single crystal In_2O_3 grown by the vapour phase technique showed promise as an anode material for the photoelectrolysis of water. Because of the potential interest in this material and its mixed oxides, several simple techniques are described here for the preparation of polycrystalline samples. Two techniques have been successfully employed. The first involves thermal evaporation and decomposition of aqueous solution of the nitrate and the second method utilizes the chemical vapour decomposition (CVD) of an appropriate organo–metallic compound, (indium acetylacetonate). While other procedures, such as the thermal decomposition of $InCl_3$ (2, 3) and sputtering (4), have been described for preparing In_2O_3 films, the behaviour of such films as anodes in the photoelectrolysis of water has not been reported.

2. Experimental details

With the first method, photoanodes were prepared by evaporating a 0.1 mol dm^{-3} solution of $In(NO_3)_3 \cdot 5H_2O$ (available from Alfa/Ventron) onto 0.5 × 0.5 cm^2 platinum squares. The latter were cleaned prior to use by an ultrasonic treatment in methanol. The platinum squares were placed on an alumina supporting plate and brought to 400° C with a Meaker burner. The indium nitrate solution was then applied dropwise to the platinum squares with care being taken to permit each drop to evaporate before applying the next. By successive evaporations multi-layer films were built up. On cooling to room temperature the films exhibited a yellow-brown colour. X-ray diffraction patterns of the films indicated that they consisted of In_2O_3. Mixed In_2O_3/Y_2O_3 oxide films were prepared by evaporating appropriate aqueous mixtures of the nitrates similar to the procedures described above.

† To whom all correspondence should be sent.

* This research was performed under the auspices of the US Department of Energy under Contract No. DE-AC02-76CH00016.

0021-891X/83 $03.00 + .12.

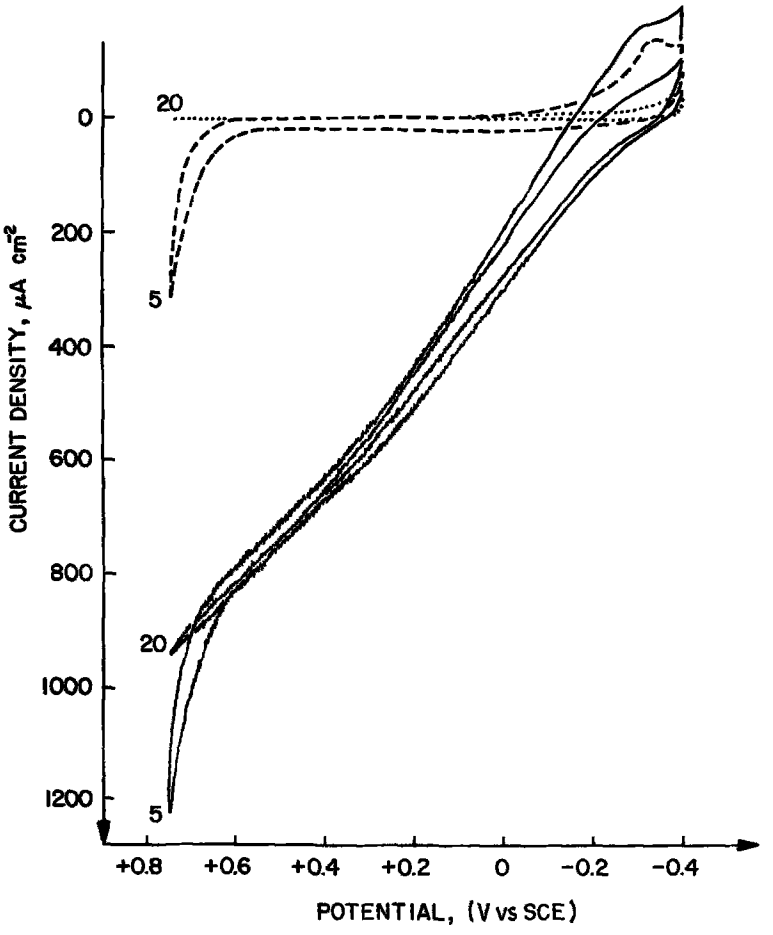

Fig. 1. I–V curves of the polycrystalline In_2O_3 with 5 and 20 deposition layers. Electrolyte 1 mol dm^{-3} NaOH, sweep rate 20 mV s^{-1}. Xenon illumination 0.2 W cm^{-2}. Dotted curves represent dark conditions.

With the CVD technique, indium acetylacetonate (Research Organic/Inorganic Corp.) was heated to 195° C and carried by a dry nitrogen stream onto platinum square foils which had been heated to 400 to 450° C.

Photocurrent voltammograms were measured as previously described [2] using a platinum foil counter electrode in an NaOH electrolyte. All potential measurements were referred to the standard calomel electrode (SCE).

3. Results

Typical voltammograms of the evaporated In_2O_3 films consisting of 5 layers and 20 layers, are shown in Fig. 1. The scan rate was 20 mV s^{-1} and the Xenon light intensity was 200 mW cm^{-2}. It is seen that the onset potential is about −0.3 V (SCE) and the photocurrent density is about 240 μA cm^{-2} at 0 V (SCE). The quantum efficiency of the polycrystalline samples compares favourably with that for the single crystal In_2O_3 (at the same applied bias) for which a photocurrent of 35 μA cm^{-2} at 25 mW cm^{-2} Xenon illumination was reported [1]. However, the effective surface areas of the polycrystalline films are higher and this may be responsible for this favourable comparison.

The photocurrent spectra of the evaporated 5 and 20 layer specimens are shown in Fig. 2. The threshold wave length is about 520 nm corresponding to an energy gap of 2.38 eV which is consistent with that reported in the paper by McCann and Bockris [1]. As expected, the photocurrent increases with applied anodic potential due to the increase in the depletion layer thickness.

The current–voltage curves of a typical CVD In_2O_3 sample is given in Fig. 3. The electrolyte was 0.1 mol dm^{-3} NaOH. The scan rate was

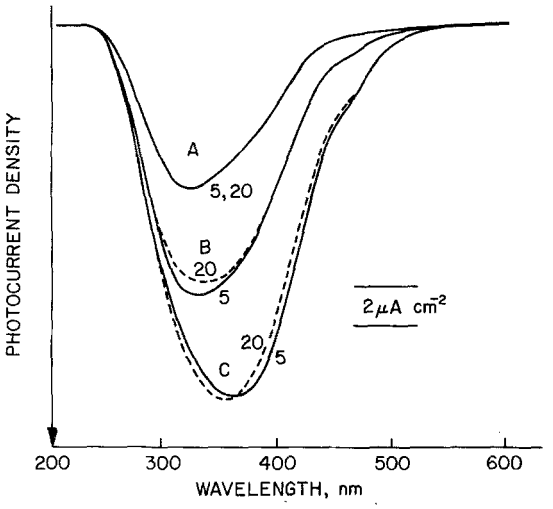

Fig. 2. Photocurrent spectra of polycrystalline In_2O_3 with 5 (solid curves) and 20 (dotted curves) deposition layers under different bias potentials. A = 0.0 V, B = 0.2 V, C = 0.4 V (SCE), respectively.

50 mV s^{-1} and the Xenon light intensity was 200 mW cm^{-2}. It is seen that the photocurrent is smaller than those of single crystal In_2O_3 and the multi-layer In_2O_3 samples discussed above. The corresponding photocurrent spectrum of the CVD sample at 0.5 V (SCE) bias potential is shown in Fig. 4. The spectral distribution differs from that shown in Fig. 2. This suggests that, depending on the method of preparation, the electronic structure of In_2O_3 may be very different. The reported electronic properties of In_2O_3 are very diverse [1, 3–5] which may be due to the mutli-valence states of the indium.

The relatively small negative value of the onset potential prompted some investigations into means for improving this property (i.e. achieving a more negative value), since the onset potential determines the required external bias. The flatband

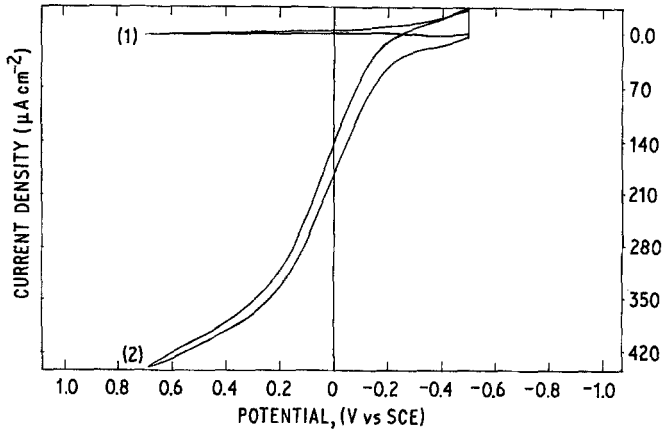

Fig. 3. Cyclic voltammogram of CVD n-In_2O_3 on platinum substrates. Sweep rate 50 mV s^{-1}; electrolyte 0.1 mol dm^{-3} NaOH. Illumination intensity 200 mW cm^{-2}. (1) represents I–V behaviour under dark. (2) represents I–V behaviour under illumination.

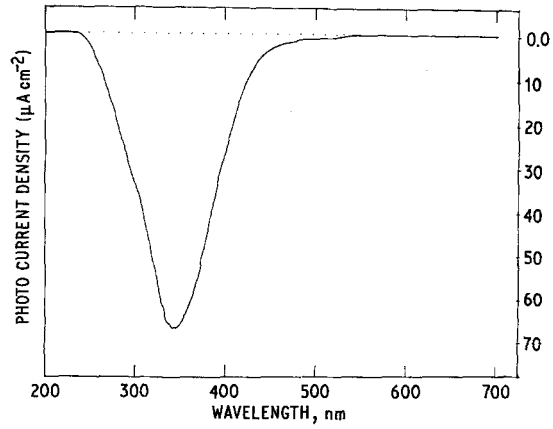

Fig. 4. Photoresponse spectrum of n-In_2O_3 (CVD on platinum substrate), taken at + 0.5 V (vs SCE) in 0.1 mol dm^{-3} NaOH. Illumination intensity 250 mW cm^{-2} before insertion of monochromator.

potential (V_{fb}), which is closely related to the onset potential, is expected to become more negative as the electron affinity (EA) of the semiconductor decreases according to the expression [6]:

$$V_{fb} = EA + \Delta E_{fc} - E_0 + V_H \qquad (1)$$

where ΔE_{fc} is the potential difference between the Fermi level and the bottom of the conduction band, V_H is the potential drop across the Helmholtz layer and E_0 is the potential of the calomel electrode relative to the vacuum level (4.75 V for SCE).

The electron affinity of the oxide semiconductor is given by;

$$EA = \chi(SC) - 1/2\, E_g \qquad (2)$$

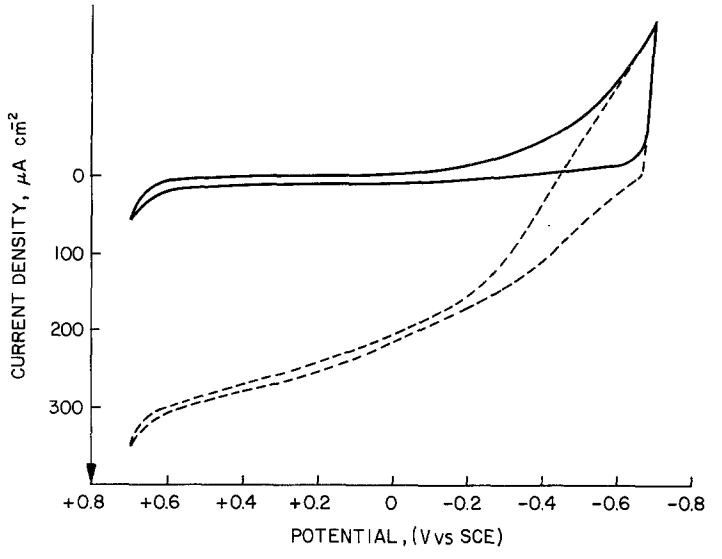

Fig. 5. I–V curves of the In_2O_3·40% · Y_2O_3 solid solution electrode. Electrolyte 1 mol dm^{-3} NaOH, sweep rate 20 mV s^{-1}. Solid curve under dark. Dotted curve under illumination. Xenon illumination 0.2 W cm^{-2}.

where E_g is the energy gap and χ(SC) is the electronegativity of the semiconductor. The latter is usually estimated by taking the geometric mean of the Mulliken electronegativities of the constituent atoms. With the above expressions in mind, consideration was given to Y_2O_3 since the atomic electronegativity of yttrium is less than that of indium [7] and the energy gap in the mixed oxide employed here is about the same as In_2O_3.

Pure Y_2O_3 tends to be very stoichiometric with a high resistance. However, the two oxides form solid solutions over the entire compositional range [9]. Several mixed In_2O_3/Y_2O_3 oxides were prepared by the previously described evporation technique. A typical voltammogram is shown in Fig. 5 for a 40% Y_2O_3/60% In_2O_3 sample. As expected, the onset potential shifted to -0.6 V as compared to -0.3 V for pure In_2O_3. However, there was a reduction in photo-

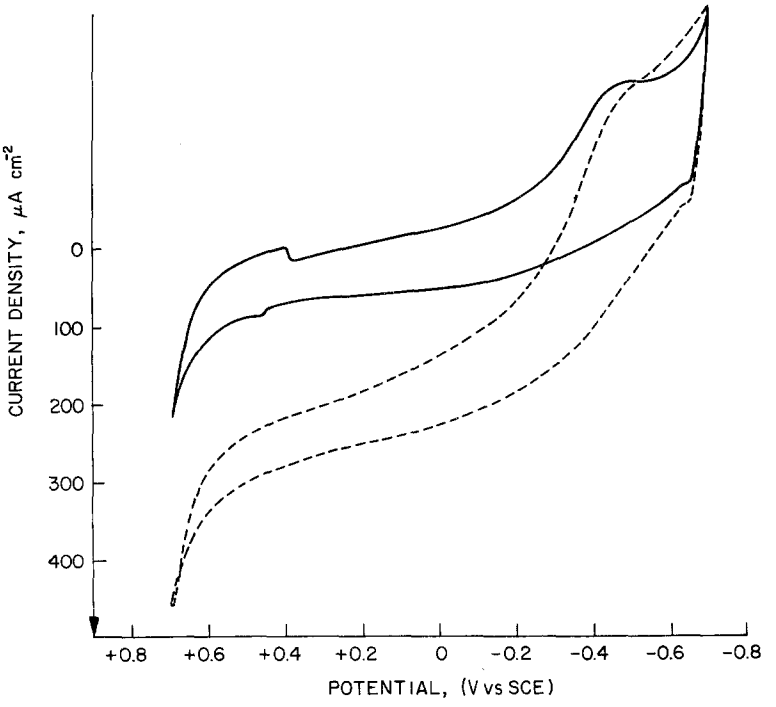

Fig. 6. I–V curves of the polycrystalline In_2O_3·40% Y_2O_3 solid solution electrode after 20 min operation. Solid curve under dark. Dotted curve under illumination.

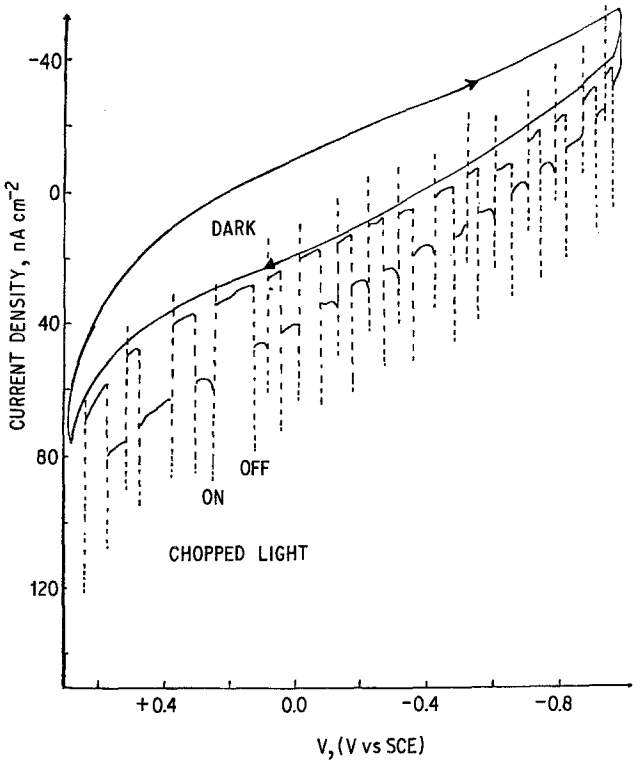

Fig. 7. I–V curves of the thermally grown Y_2O_3 from firing yttrium foil at 500° C for 25 min. Electrolyte 1 mol dm^{-3} NaOH, sweep rate 50 mV s^{-1}. Xenon illumination 0.200 mW cm^{-2}.

current (at 200 mW cm^{-2} Xenon illumination) and the sample showed some evidence of corrosion after a short period of operation. On continued operation for 20 min with the electrode biased at zero volt (SCE), the I–V curves (Fig. 6) changed shape and new redox peaks appeared. Furthermore, the surface of the sample was markedly corroded.

It should be mentioned that efforts have been made to improve the conductivity of Y_2O_3 by adding impurities. Metal oxides such as RuO_2, MnO_2, Nb_2O_5, V_2O_5, Fe_2O_3, and PbO_2 were used for this purpose. These powder oxides were well mixed with Y_2O_3 powder at about 0.01 to 1 at % and then sintered at 1400° C for 10 h. Unfortunately, all of these samples still showed a very large resistance and no photoeffect was detected.

For purposes of reference, Y_2O_3 anodes were prepared by firing yttrium foil (Alpha-Ventron Supplier) with a Meaker burner at 500 to 1000° C over a period of 20 s to 30 min. All samples exhibited a high resistance (10^7 Ω). The voltammetry curves for a sample prepared by heating to 500° C for 25 min is shown in Fig. 7. Chopped Xenon illumination (200 mW cm^{-2}) was employed. A large transient current was noted and is probably associated with a high recombination rate.

Heat treatment of Y_2O_3 in a reducing atmosphere (e.g. H_2) does not improve the electrical conductivity. It has been reported that non-stoichiometric Y_2O_3 exhibits p-type conductivity [10, 11]. Work is underway to improve the n-type conductivity of Y_2O_3 by ion implanation.

References

[1] J. F. McCann and J. O'M. Bockris, *J. Electrochem. Soc.* **128** (1981) 1719.
[2] A. Raza, O. P. Agnihotri and B. K. Gupta, *J. Phys. D.* **10** (1977) 1871.
[3] H. Kostlin, R. Jost and W. Lems, *Phys. Status Solidi* **29** (1975) 87.
[4] W. W. Molzen, *J. Vac. Sci. Technol.* **12** (1975) 99.
[5] F.-T. Liou, C. Y. Yang and S. N. Levine, *J. Electrochem. Soc.* **129** (1982) 342.
[6] C. A. Pan and T. P. Ma, *J. Electronic Mater.* **10** (1981) 43.
[7] R. L. Weiher and R. P. Ley, *J. Appl. Phys.* **37** (1966) 299.
[8] E. Y. Wang and L. Hsu, *J. Electrochem. Soc.* **125** (1978).
[9] M. A. Butler and D. S. Ginley, *ibid.* **125** (1978) 228.

[10] Alfa Catalog 1980–81, Thiokol/Ventron Division, Danvers, Mass. p. Y-36, Y-96.
[11] W. H. Nebergall, F. C. Schmidt and H. F. Holtzclaw, Jr. 'College Chemistry', D. C. Heath and Co. (1963) p. 72.
[12] S. J. Schneider, R. S. Roth and J. L. Waring, *J. Res. Nat. Bur. Stand.* 65A (1961) 372.
[13] Per Kofstad, 'Nonstoichiometry, Diffusion, and Electrical Conductivity in Binary Metal Oxides', 'Wiley-Interscience, New York (1972).